

Mott insulating and glassy phases of polaritons in 1D arrays of coupled cavities

Davide Rossini¹ and Rosario Fazio^{2,1}

¹*NEST-CNR-INFM & Scuola Normale Superiore, Piazza dei Cavalieri 7, I-56126 Pisa, Italy*

²*International School for Advanced Studies (SISSA), Via Beirut 2-4, I-34014 Trieste, Italy*

By means of analytical and numerical methods we analyze the phase diagram of polaritons in one-dimensional coupled cavities. We locate the phase boundary, discuss the behavior of the polariton compressibility and visibility fringes across the critical point, and find a non-trivial scaling of the phase boundary as a function of the number of atoms inside each cavity. We also predict the emergence of a *polaritonic glassy phase* when the number of atoms fluctuates from cavity to cavity.

Over the past two decades a considerable understanding of the physics of strongly interacting systems has been gained by a judicious design of controlled many-body systems. Successful examples of this sort were optical lattices or Josephson junction arrays (see the reviews [1, 2]). The recent proposals [3, 4, 5] to realize a Mott phase of polaritons have paved the way to use coupled cavities for the study of strongly correlated phenomena in a controlled way. The rich scenario which emerges in these systems stems from the interplay of two effects. Light-matter interaction inside the cavity leads to a strong effective Kerr nonlinearity between photons. By controlling the atomic level spacings and the photonic resonance frequency inside the cavity, it is possible to achieve a photon blockade regime [6, 7, 8, 9], thus suppressing photon fluctuations in each cavity. On the other hand, photon hopping between neighboring cavities favours delocalization thus competing with photon blockade. Coupled cavities can be realized in a wide range of physical systems, from nanocavities in photonic crystals [10] to Cooper pair boxes in superconducting resonators [11]. It is therefore possible to study a whole new class of strongly interacting systems that, for the first time, can be addressed and measured locally.

The polariton Mott insulator has been predicted in two cases. Hartmann *et al.* [3] discussed a cavity doped with N four-level systems in the limit of large N , while Angelakis *et al.* [5] and Greentree *et al.* [4] analyzed the Jaynes-Cummings [12] model as a scheme for the light-matter interaction; in this last case, an experimental proposal has been also devised by Neil Na *et al.* [13]. Hartmann *et al.* found a mapping onto a Bose-Hubbard model [14] for the polaritons in the limit of large number of atoms and large detuning. In the other case, the phase boundary was evaluated at a mean field level for one [4] and many [13] atoms in cavity. The exact phase diagram has not been worked out so far; this is what we accomplish in this work for the one-dimensional case. By means of numerical simulations and analytical calculations we are able to locate the phase boundary and its non-trivial scaling as a function of the number of atoms in the cavity. Furthermore we consider the case where the number of atoms fluctuates in each cavity and we show that this leads to the existence of a polariton glass.

The Hamiltonian for the system composed by an array of L identical coupled cavities is given by the local Hamiltonian on each cavity and the photon hopping term between different cavities:

$$\mathcal{H} = \sum_{i=1}^L \mathcal{H}_i^{(a)} - t \sum_{\langle i,j \rangle} (a_i^\dagger a_j + a_j^\dagger a_i) - \mu \sum_{i=1}^L n_i. \quad (1)$$

As in [4, 13], we add a chemical potential μ . In the previous expression t is the nearest-neighbor inter-cavity photon hopping, and a_i is the photon annihilation operator in the i -th cavity; the local contribution $\mathcal{H}_i^{(a)}$ describes the light-matter interaction. We will consider the following two models.

Model I A collection of N two-level systems which interact with photons via a Jaynes-Cummings coupling $\mathcal{H}_i^{(I,a)} = \epsilon(S_i^z + \frac{N}{2}) + \omega a_i^\dagger a_i + \beta(S_i^+ a_i + S_i^- a_i^\dagger)$, where we have defined the spin operators $S_i^\alpha = \sum_{j=1}^N \sigma_{j,i}^\alpha$ ($\alpha = \pm, z$) and $\sigma_{j,i}^\pm$ are the atomic raising/lowering operators for the j -th atom, ϵ denotes the transition energy between the two atomic levels, ω is the resonance frequency of the cavity, and β is the atom-field coupling constant ($\epsilon, \omega, \beta > 0$). The total number of atomic plus photonic excitations and the total atomic spin S_i^z on each site are conserved quantities. The ground state is always in the subspace of maximum spin, $S = N/2$.

Model II In the Jaynes-Cummings model at a large detuning Δ , when the atomic spontaneous emission is minimized, also the strength of nonlinearities is weakened. In order to overcome this problem, a different scheme involving four-level atoms, has been proposed [15] producing a large Kerr nonlinearity with virtually no noise. In the interaction picture, in electric dipole and rotating wave approximations the model reads $\mathcal{H}_i^{(II,a)} = \delta S_i^{33} + \Delta S_i^{44} + \Omega(S_i^{23} + S_i^{32}) + g_1(S_i^{13} a^\dagger + S_i^{31} a) + g_2(S_i^{24} a^\dagger + S_i^{42} a)$, having defined the global atomic raising and lowering operators $S^{lm} = \sum_{j=1}^N |l\rangle_j \langle m|$; $\sigma_j^{lm} = |l\rangle_j \langle m|$ are the atomic raising and lowering operators ($l \neq m$), or energy level populations ($l = m$) for the j -th atom. The transition $|3\rangle_j \rightarrow |2\rangle_j$ is driven by a classical coupling field with Rabi frequency Ω ; the cavity mode of frequency ω_{cav} couples the $|1\rangle_j \rightarrow |3\rangle_j$ and $|2\rangle_j \rightarrow |4\rangle_j$ transitions with coupling constants g_1 and g_2 ; the parameters δ and Δ account for the detunings of

levels 3 and 4 respectively. The atomic part of the system wavefunction for the i -th cavity can be fully characterized by the number of atoms in each of the four possible states: $\{|n_1, n_2, n_3, n_4\rangle\}$, with $\sum_{i=1}^4 n_i = N$. The total number of photons plus the number of atomic excitations in the whole system (where states $|2\rangle_j, |3\rangle_j$ count for one excitation, while $|4\rangle_j$ counts for two excitations), is a conserved quantity. Hereafter we assume $g_1 \simeq g_2 \equiv g$ and define the relative atomic detuning $\delta_w \equiv \Delta - \delta$.

Mott insulator The phase diagram of the coupled cavity system is characterized by two distinct phases [3, 4, 5]: the Mott Insulator (MI) is surrounded by the Superfluid (SF) phase. In the MI polaritons are localized on each site, with a uniform density $\rho \equiv n^{pol}/L$, where n^{pol} is the total number of polaritons in a system of L cavities; there is a gap in the spectrum, and the compressibility $\kappa \equiv \partial\rho/\partial\mu$ vanishes. A finite hopping renormalizes this gap, which eventually vanishes at t^* . The phase boundaries between the two phases can thus be determined by evaluating, as a function of the hopping, the critical values of μ at which the gap vanishes. Our data have been obtained by means of the Density Matrix Renormalization Group (DMRG) algorithm with open boundary conditions [16]. In numerical calculations, the Hilbert space for the on-site Hamiltonian is fixed by a maximum number of admitted photons n_{\max}^{phot} . We chose $n_{\max}^{phot} = 6$ for model *I* and $n_{\max}^{phot} = 4$ for model *II*; we also retained up to $m = 120$ states in the DMRG procedure, such to guarantee accurate results, and checked that our data are not affected by increasing n_{\max}^{phot} . We simulated systems with up to $L = 128$, and up to $N = 5$ atoms per cavity [17]; the asymptotic values in the thermodynamic limit have been extracted by performing a linear fit in $1/L$. By combining these results with strong coupling perturbation theory [18] we were able to locate the phase boundaries for all values of N . Most of this paper is devoted to the case $\epsilon = \omega$ for model *I* and $\delta = \Delta = 0$ for model *II*. These regimes could not be accessed by the perturbative approach of Ref. [3].

Let us start with zero photon hopping ($t = 0$). For model *I*, at fixed N , there exists a value δ_I^* of the detuning $\delta_I \equiv \omega - \epsilon$ such that, for $\delta_I > \delta_I^*$, the width of the lobe with a polaritonic density $\rho = N$ is greatly enhanced with respect to the other lobes. We estimate δ_I^* numerically and find a scaling $\delta_I^* \sim \sqrt{N}$. For model *II*, at a given relative atomic detuning $\delta_w > 0$ the situation is similar to model *I*, where the resonating lobe with $\rho = N$ is much larger than the other lobes, if $\delta < \delta^*$. In the opposite case, $\delta_w < 0$, some of the lobes disappear.

For model *I*, numerical data at finite photon hopping for different values of N are shown in Fig. 1; the phase diagram of model *II* is shown in Fig. 2. Several interesting features emerge in the structure of the lobes. In both models, for fixed N , contrary to Bose-Hubbard model, the critical values t^* of the hopping strength at which the various lobes shrink in a point are not proportional

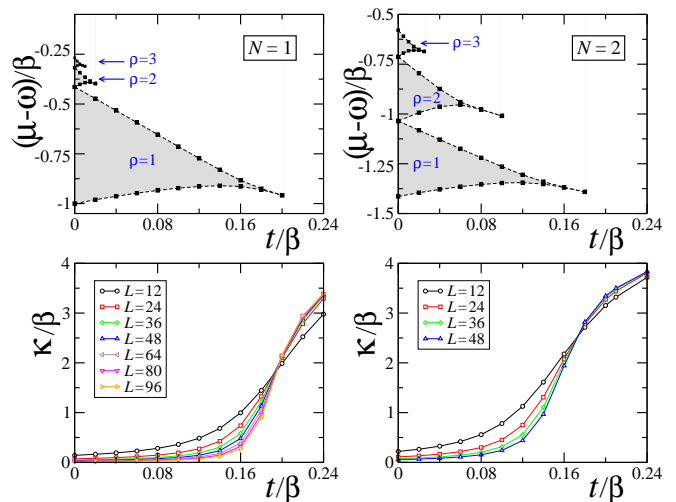


FIG. 1: (Color online) Upper panels: Phase diagram for the Hamiltonian model *I*, with $N = 1, 2$ atoms inside each cavity at $\epsilon = \omega$. Lower panels: System compressibility κ for the first lobe (i.e., $\rho = 1$), for different system sizes L , with $N = 1$ (left) and $N = 2$ (right).

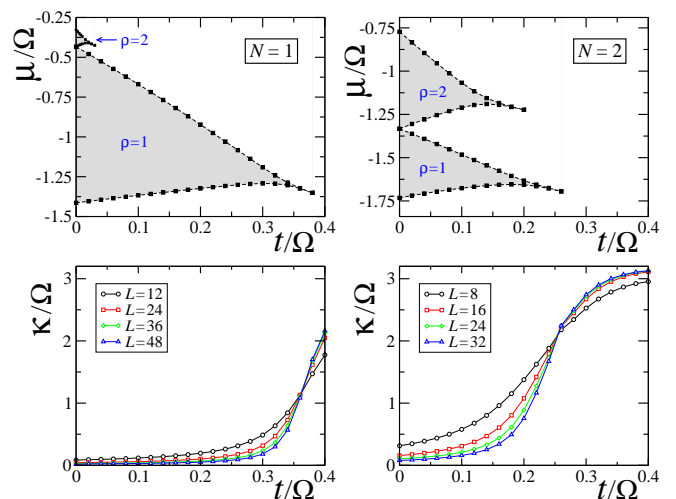


FIG. 2: (Color online) Upper panels: Phase diagram of model *II*. The detuning parameters are set to zero and $g/\Omega = 1$. Lower panels: System compressibility κ for the first lobe, for different system sizes L , with $N = 1$ (left) and $N = 2$ (right).

to the lobe width at $t = 0$. Furthermore, the ratio between the upper and the lower slopes of the lobes at small hopping is greater than the one predicted in Ref. [18]; this discrepancy disappears on increasing the number of atoms inside the cavity. In terms of an effective Bose-Hubbard model, this may be understood as a *correlated hopping* of the polaritons, i.e., the hopping depends on the occupation of the cavity.

A more detailed analysis of the transition at filling one can be performed by considering the compressibility. In

our DMRG simulations we fix the total number n^{pol} of excitations in the system, thus fixing the polariton density ρ inside each cavity in the insulating regime. In the lower panels of Figs. 1, 2 we plot κ in the first insulating lobe (with a polariton density $\rho = 1$) as a function of t for different sizes of the system, for the models *I* and *II*. By exploring the mapping to the Bose-Hubbard model we construct the full curve t^* versus N . The effective repulsive interaction U_{eff} between polaritons, at $\rho = 1$, is given by $U_{\text{eff}}(1) \equiv \partial^2 E(n)/\partial n^2|_{n=1}$ (where $E(n)$ is the ground state energy of Hamiltonian \mathcal{H}_i with n polaritons), that is exactly the opening of the first lobe at $t = 0$. For model *I* it is possible to give an exact analytic formula: $U_{\text{eff}}(1) = 2\sqrt{N}[1 - \sqrt{1 - 1/(2N)}]$, while for model *II* it can be evaluated numerically. As N increases, $U_{\text{eff}}(1)$ decays to zero; for both models $U_{\text{eff}}(1) \sim 1/\sqrt{N}$ as far as $N \rightarrow \infty$. Moreover the effective repulsion depends on the number of polaritons, contrary to the Bose-Hubbard model; this dependence weakens, and eventually vanishes in the limit $n \ll N$. Therefore the mapping becomes accurate when N increases. The polaritonic hopping t_{eff} can be obtained by performing a strong coupling expansion in t . For model *I* we found that $t^* \sim 2t_{\text{eff}}^*$, while for model *II* we get $t^* \sim 2\frac{N+1}{N}t_{\text{eff}}^*$. The critical hopping is then obtained using the value for the critical point $t_{\text{eff}}^*/U_{\text{eff}} \simeq 0.3$ [19]. Figure 3 (upper part) displays both numerical (blue squares) and analytical estimates (red circles) for the two models. This analysis shows that the Bose-Hubbard model provides a good description already for $N \sim 10$. A study of the dynamics is needed to further strengthen this observation. We point out that, in experimental realizations, the parameter that can be changed to cross the transition is the detuning. For model *I* this is shown in the lower part of Fig. 3.

Visibility of photon interference The phase transition can be detected by analyzing the phase coherence of photons [21], in a way similar to what has been done for the Bose-Hubbard model [21, 22]. The interference pattern of the photonic density is proportional to the photon number distribution \mathcal{S} in the momentum space: $\mathcal{S}(k) = \frac{1}{L} \sum_{j,l=1}^L e^{2\pi i k(j-l)/L} \langle a_j^\dagger a_l \rangle$. The visibility of interference fringes can then be defined as $\mathcal{V} = (\mathcal{S}_{\text{max}} - \mathcal{S}_{\text{min}})/(\mathcal{S}_{\text{max}} + \mathcal{S}_{\text{min}})$. The visibility is strictly zero only in the limit $t = 0$, where the interference pattern \mathcal{S} is constant. When t is increased, the visibility itself increases, until it saturates to the maximum value $\mathcal{V} = 1$ in the superfluid regime. This description is well adapted even for photon coherence in our hybrid light-matter system, as shown in Fig. 4. The existence of different phases can also be detected by measuring fluctuations in the number of polaritons, as discussed in [3].

Polaritonic glass phase Up to now we have assumed that the number of atoms in each cavity was constant and equal to N . In certain implementations this requirement might be demanding. Here however we consider this problem from a different perspective and show that,

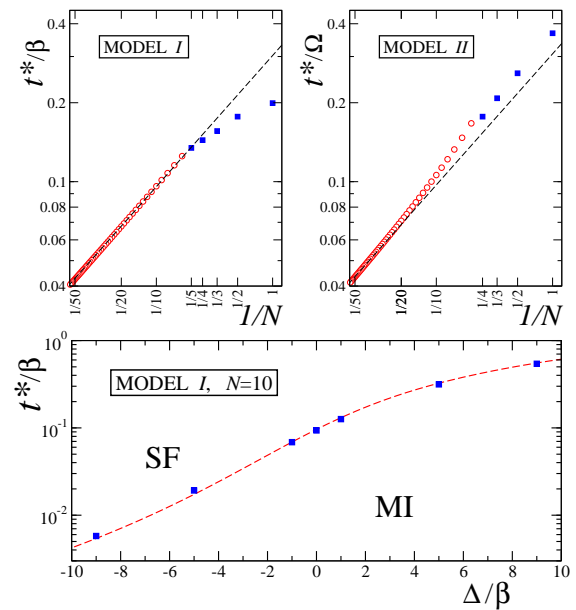


FIG. 3: (Color online) Upper graphs: Critical hopping t^* in the first lobe as a function of the number N of atoms inside each cavity, for the two different models with all the detunings set to zero. Dashed black lines indicate a behavior $t^* \sim 1/\sqrt{N}$ and are plotted as guidelines. Lower graph: Critical hopping t^* for model *I* with $N = 10$ atoms per cavity [20], as a function of the relative detuning Δ . Blue squares have been evaluated with the DMRG. Red data are estimates obtained from the effective on-site polaritonic repulsion U_{eff} at zero hopping, with filling $\rho = 1$.

when N changes from cavity to cavity, it leads to the emergence of a *polariton glass*. Following [14], this phase is characterized by a finite compressibility, gapless excitation spectrum, and zero superfluid density.

Random fluctuations in the number of atoms per cavity lead to disorder in the on-site light-matter interaction strength. This effect can cause significant consequences only in the limit of large N (we quantify this statement below) where the mapping onto a Bose-Hubbard model applies. A Bose glass phase has been originally predicted [14] as a function of disorder in the chemical potential. Recently it has been shown that fluctuations in the on-site repulsion lead to a Bose glass as well [23].

We take advantage of the results obtained in [23] and the mapping to an effective Bose-Hubbard model to give a detailed estimate for the width of the polariton glass phase. The key to our finding is to relate fluctuations in the number of atoms to fluctuations in the on-site repulsion U_{eff} . We suppose that each N_i is a random discrete Gaussian variable with a mean value $\langle N \rangle$, and a standard deviation δN . Figure 5 displays fluctuations in the effective on-site repulsion δU_{eff} as a function of the fluctuations in the number of atoms, while in the inset of Fig. 5 we show an example of such a varia-

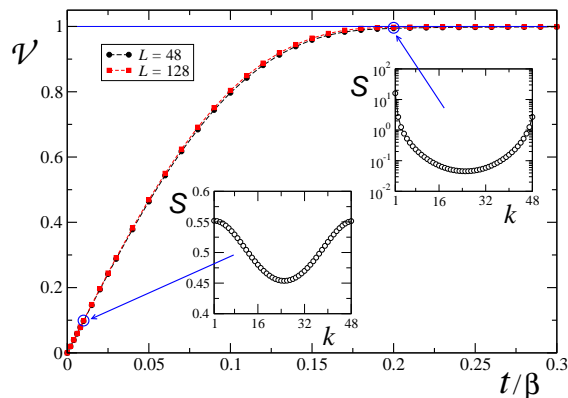


FIG. 4: (Color online) Photonic visibility \mathcal{V} in the first insulating lobe ($\rho = 1$) as a function of the hopping strength t/β , for model *I*. Here we considered the case $N = 1$, $\Delta = 0$. Insets: The photon number correlation function $\mathcal{S}(k)$ for $L = 48$ in the deep insulating regime ($t/\beta = 0.01$), and at the edge of the superfluid regime ($t/\beta = 0.20$).

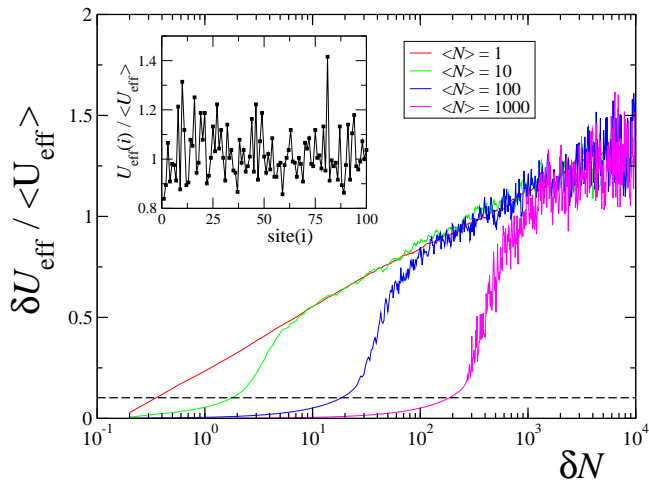


FIG. 5: (Color online) Relative standard deviation of the effective on-site interaction strength U_{eff} averaged over $L = 10^4$ cavities, as a function of the atom number fluctuations δN ; from left to right $\langle N \rangle = 1, 10, 100, 1000$. Dashed line indicates an effective variation of the interaction strength equal to the standard deviation of a random interaction uniformly distributed in the interval $U_{\text{eff}}(i) / \langle U_{\text{eff}} \rangle \in [-\epsilon, +\epsilon]$ with $\epsilon = 0.25$. In the inset an example of the variation on the on-site effective interaction is shown; $\langle N \rangle = 100$, $\delta N = 20$.

tion, with $\langle N \rangle = 100$, $\delta N = 20$, in the case of model *I*. We can then use numerical data of Ref. [23] to estimate where the polaritonic glass phase can be observed. It has been shown that in the Bose Hubbard model, for a relative interaction $\delta U_{\text{eff}} / \langle U_{\text{eff}} \rangle$ uniformly distributed in an interval of length $2\epsilon = 0.5$, a $L = 200$ sites system at filling $\rho = 1.01$ exhibits a Bose glass phase for $0.078 \lesssim t_{\text{eff}} / \langle U_{\text{eff}} \rangle \lesssim 0.133$. In our model with the same polaritonic filling, if we take, e.g., $\langle N \rangle = 100$ particles per

cavity and we choose $\delta N \simeq 19$ (such to have $\epsilon = 0.25$), a polaritonic glassy phase should be visible, in the case of model *I*, for $7.51 \times 10^{-3} \lesssim t/\beta \lesssim 1.401 \times 10^{-2}$. The situation is qualitatively the same for model *II*. The polaritonic glass may be observed by measuring, at fractional fillings, the photon visibility as a function of the disorder. Anyway, a complete characterization of the polaritonic glass requires a study of its dynamical behavior.

Concluding remarks In this work we have discussed in details the equilibrium properties of a chain of coupled cavities. The results we presented here are general, in the sense that they apply to all the systems described by Eq. (1). An important issue is to understand the effect of decoherence, decay, cavity losses, . . . , which occur in these systems. These aspects have to be discussed for each implementation (see for example [3, 11]), together with the effect of an additional possible external driving. The combined presence of dissipation and external driving may lead to a change of the universality class of the transition, or to new phenomena associated to non-equilibrium phases.

We acknowledge useful discussions with A. Tredicucci and support by MIUR-PRIN and EC-Eurosqip.

-
- [1] M. Lewenstein *et al.*, *Adv. Phys.* **56**, 243 (2007).
 - [2] R. Fazio and H. van der Zant, *Phys. Rep.* **355**, 235 (2001).
 - [3] M.J. Hartmann, F.G.S.L. Brandão, and M.B. Plenio, *Nature Physics* **2**, 849 (2006).
 - [4] A.D. Greentree *et al.*, *Nature Physics* **2**, 856 (2006).
 - [5] D.G. Angelakis, M.F. Santos, and S. Bose, *Phys. Rev. A* **76**, 031805(R) (2007).
 - [6] A. Imamoglu *et al.*, *Phys. Rev. Lett.* **79**, 1467 (1997).
 - [7] S. Rebić *et al.*, *J. Opt. B: Quantum Semiclass. Opt.* **1**, 490 (1999).
 - [8] J. Kim *et al.*, *Nature* **397**, 500 (1999).
 - [9] K.M. Birnbaum *et al.*, *Nature* **436**, 87 (2005).
 - [10] Y. Akahane *et al.*, *Nature* **425**, 944 (2003).
 - [11] A. Wallraff *et al.*, *Nature* **431**, 162 (2004).
 - [12] B.W. Shore and P.L. Knight, *J. Mod. Opt.* **40**, 1195 (1993).
 - [13] Y.C. Neil Na *et al.*, [quant-ph/0703219](http://arxiv.org/abs/quant-ph/0703219).
 - [14] M.P.A. Fisher *et al.*, *Phys. Rev. B* **40**, 546 (1989).
 - [15] H. Schmidt and A. Imamoglu, *Opt. Lett.* **21**, 1936 (1996).
 - [16] The DMRG code of the “Powder with Power” project (<http://www.qti.sns.it>) has been used.
 - [17] In model *II*, for $N = 3, 4$, only states with at most three atomic excitations and $n_{\text{max}}^{\text{phot}} = 3$ were considered.
 - [18] J.K. Freericks and H. Monien, *Phys. Rev. B* **53**, 2691 (1996).
 - [19] T.D. Kühner, S.R. White, and H. Monien, *Phys. Rev. B* **61**, 12474 (2000).
 - [20] For $N = 10$ we limited the total polariton number per site to $n = 4$.
 - [21] M.X. Huo *et al.*, [quant-ph/0702078](http://arxiv.org/abs/quant-ph/0702078).
 - [22] F. Gerbier *et al.*, *Phys. Rev. Lett.* **95**, 050404 (2005).
 - [23] H. Gimperlein *et al.*, *Phys. Rev. Lett.* **95**, 170401 (2005).